September 20, 1990

Warsaw University Preprint *IFD/9/1990*

Multiplicity distributions in e^+e^- and pp collisions and bivariate branching process

G. Wrochna

Institute of Experimental Physics
Warsaw University
PL-00-681 Warsaw, ul. Hoża 69

Abstract

Multiparticle production is studied as a bivariate branching process: in multiplicity and in energy. In this approach the Central Limit Theorem predicts multiplicity distribution to be lognormal and obeying the KNO-G scaling. The analytical results are compared with Monte Carlo calculations. It is shown that the KNO-G scaling and the lognormal shape of the multiplicity distributions are well established features of experimental e^+e^- and pp data as well as those generated by Monte Carlo programs.

Talk given at the XX International Symposium on Multiparticle Dynamics, Gut Holmecke, Germany, September 1990.

1 Introduction

The experimentally observed multiplicity distributions in e^+e^- and pp inelastic collisions are characterized by the three basic features: the shape of the distributions is lognormal, the distributions obey the scaling, and the average multiplicity depends on the energy according to a power law. The experimental evidence for these features is presented in Sections 2 and 3. Sections 4, 5, and 6 are devoted to a possible explanation of the observed facts. The study presented here was done in collaboration with R.Szwed and A.K.Wróblewski.

2 e^+e^- collisions

The lognormal shape of the distributions and the scaling law can be described by the following formulae:

$$P_n = \int_{n/\langle n\rangle}^{(n+1)/\langle n\rangle} \psi(z)dz \ , \tag{2.1}$$

$$\psi(z) = \frac{N}{\sqrt{2\pi}\sigma} \cdot \frac{1}{z+c} \exp\left(-\frac{[\ln(z+c)-\mu]^2}{2\,\sigma^2}\right) . \tag{2.2}$$

To avoid strong correlation between μ and σ it is better to fit the shift c and the dispersion $D = \sqrt{\langle z^2\rangle - \langle z\rangle^2}$ and calculate N, μ and σ from normalization conditions [1]

$$\int_0^\infty \psi(z)dz = \int_0^\infty z\psi(z)dz = 1 \ . \tag{2.3}$$

The global fit to the e^+e^- data for $\sqrt{s}$ between 7 and 91 GeV (including recently published data from TRISTAN and LEP) gives [2]

$$c = 0.56 \pm 0.03, \quad D = 0.277 \pm 0.001 \quad \chi^2/NDF = 208/285 = 0.74 \tag{2.4}$$

$$(N = 1.000 \quad \mu = 0.429 \quad \sigma = 0.1762) \ .$$

The goodness of the fit is shown in Fig. 1 which is a probit diagram [1,3,4]. An alternative test of the scaling is presented in Fig. 2 where dispersions of various orders $D_k = \sqrt{\langle n_{ch}^k\rangle - \langle n_{ch}\rangle^k}$ are plotted as functions of the average multiplicity $\langle n_{ch}\rangle$. It is seen that the dependences of D_k on $\langle n_{ch}\rangle$ are linear which proves the scaling. The continuous lines drawn in the figure are calculated from the lognormal distribution with parameters (2.4).

To make the most direct test of the scaling we have fitted each of data sets separately. The resulting parameters are presented in Fig. 3. It is seen that the parameters from various experiments are slightly different, but do not show any systematic dependence on the energy. Thus all observed multiplicity distributions in e^+e^- collisions can be described by a single lognormal distribution with two parameters fixed for all energies.

Fig. 4 presents the dependence of the average multiplicity $\langle n_{ch}\rangle$ on the collision energy $\sqrt{s}$. The continuous line represents the power law $\langle n_{ch}\rangle = 1.48 \cdot s^{0.221}$ [5] which describes the data quite well.

3 pp inelastic collisions

Multiplicity distributions in pp collisions have similar properties to those observed in e^+e^- interactions[1]. Figure 5 – a probit diagram – proves the scaling and the lognormal shape of

[1]The pp nondiffractive collisions were independently studied in Ref. [6].

the distributions in the range from $\sqrt{s} = 3$ to 62 GeV. The dispersions of various orders are plotted in Fig. 6. Figure 7 presents the values of parameters c and D fitted to each of data sets separately. It is seen that all data in the range from $\sqrt{s} = 3$ to 62 GeV can be described by a common lognormal distribution [7]

$$c = 4.25 \pm 0.20, \quad D = 0.629 \pm 0.003 \quad \chi^2/NDF = 458/316 = 1.45 \tag{3.1}$$

$$(N = 1.061 \quad \mu = 1.638 \quad \sigma = 0.1210).$$

Only the UA5 data at 540 GeV require different parameters [7] (Fig. 8)

$$c = 1.12 \pm 0.22, \quad D = 0.642 \pm 0.011 \quad \chi^2/NDF = 29/38 = 0.77 \tag{3.2}$$

$$(N = 1.028 \quad \mu = 0.692 \quad \sigma = 0.3003).$$

However we would like to stress that the observed scaling violation in inelastic data at this energy is significantly smaller than that in nondiffractive collisions which is usually quoted.

It is well known that the dependence of the average multiplicity on the energy in pp collisions is similar to that in e^+e^- interactions. It was shown [7] that it also obeys the power law with the same exponent. It is seen in Fig. 9 where the horizontal axis corresponds to $W = \sqrt{s}$ for e^+e^- and $W = (\sqrt{s} - 2m_p)\ /\ 3$ for pp. It suggests that pp collisions can be treated as a certain combination of e^+e^- collisions. Usually two scenarios are considered.

Scenario 1. Only one parton from each proton is engaged in the reaction, whereas the remaining partons are only "spectators". Thus, the colliding partons create a cascade similar to that in the e^+e^- collisions. However, the spectators remove a part of the energy so that the initial energy of the cascade varies from event to event. Thus the final distribution is a mixture of the elementary distributions with various initial energies.

Scenario 2. The initial energy is divided between a number of colliding parton pairs. Each pair develops an elementary cascade. Thus the final distribution is a convolution of several elementary distributions.

It was shown [7] that any combination of both scenarios saves the scaling and the power law for the average multiplicity.

4 Bivariate branching

The multiparticle production is recently often studied as a stochastic branching process. This study started in 1970 when Polyakov [8] showed that the branching picture of multiparticle production is implicated by the scale-invariant field theory with the similarity principle. Since that time many approaches were proposed to calculate final multiplicity distributions. The important feature of our approach is that the process is controlled by two variables having the same rank, the multiplicity and the parton energy, rather than by the multiplicity only. It is illustrated in Fig. 10 where the thickness of a branch represents the energy available for particle production carried by a given parton.

5 Particle production as a random walk

Let me illustrate the process in the following graph (Fig. 11). Let the vertical axis correspond to the multiplicity n, and the horizontal axis — to the average energy E available for particle production carried by a single parton (it is sometimes called "cluster mass"). The process starts from $E = \sqrt{s}$ and $n = 1$ and ends at E of the order of the pion mass and a certain value of multiplicity. In each step the number of particles increases and the energy of each particle decreases, thus the process is a kind of random walk in multiplicity and energy. Because of the multiplicative version of the Central Limit Theorem the probability of walking from a given point to another one is given by the bivariate lognormal distribution which is shown in

Fig. 11 as a contour plot. If we want to obtain the final multiplicity distribution we should set the starting point at $n = 1$ and $E = \sqrt{s}$ and take the vertical slice at $E \approx m_\pi$. Thus we see that the final multiplicity distribution is lognormal. If we start from various values of $\sqrt{s}$ then the final distribution is given by various vertical slices. That is the reason of scaling. It also determines that the average multiplicity depends on the energy as $\langle \tilde{n} \rangle = \beta s^\alpha$. The details of the calculation can be found in Ref. [5].

It is interesting to note that such a picture of multiparticle production implies also the lognormal distribution of the final particle energy. Thus the observation of the OPAL collaboration (this conference) that the distribution of the momentum of charged particles is close to the lognormal one is one more confirmation of the presented picture.

This picture can be easily generalized for pp collisions. The initial interaction (scenario 1 and 2) can be treated as a first step of the branching. Of course this step has slighly different properties than others but (due to the Central Limit Theorem) it can only change the parameters of the final distributions.

6 "Poor Man's" Monte Carlo

The crucial point of the Central Limit Theorem is that the final results depend on the general scheme of the process rather than on any details concerning individual steps. To illustrate this fact in case of bivariate branching let me present you a very simple Monte Carlo example. I will use words such as "particle", "energy", "decay" etc., but I will have in mind abstract mathematical quantities and formulae rather than real physical objects and processes.

The program starts from a single particle with a certain energy E_0. The particle decays. It means that we generate two random numbers. The first one is a fraction of the energy kE which will be – let us say – used for the movement of created particles, i.e. simply subtracted.

$$E_0' = E_0 - kE_0 \ . \tag{6.1}$$

As a distribution of k a flat distribution ranging from 0.2 to 0.8 was taken. The second number r is used to divide the rest of the energy between the two created particles.

$$E_1 = rE_0' \quad E_2 = (1-r)E_0 \ . \tag{6.2}$$

A flat distribution ranging from 0 to 1 was taken. Each of the created particles can break again until its energy is greater than a certain cut value, for example 0.28 ($2m_\pi$ in GeV).

We have generated in this way one million events for several initial energies. Obtained multiplicity distributions are presented in Fig. 12. The points from various energies form a single line which proves the excellent scaling. The continuous straight line represents the lognormal distribution fitted to the e^+e^- multiplicity data. It is seen that multiplicity distributions generated by the simple Monte Carlo have close to the lognormal shape and coincide quite well with the experimental data.

Figure 13 shows that also the experimentally observed dependence of the average multiplicity on the collision energy is reproduced very well.

It seems incredible that so primitive Monte Carlo is able to reproduce experimental results with such high precision. It is a good illustration of the predictive power of the Central Limit Theorem. Thus this example has rather mathematical than physical meaning. If we want to be closer to reality we can use a "professional" Monte Carlo programs strongly based on the QCD.

7 "Professional" Monte Carlo

We have used two Monte Carlo programs — JETSET and HERWIG and we have generated 50000 events at energies indicated in Fig. 14 and 15. The resulting multiplicity distributions

are plotted in these figures for each generator as probit diagrams. The continuous line represents the lognormal distribution fitted to the experimental e^+e^- data. It is seen that the multiplicity generated by JETSET has the lognormal shape, obeys the scaling and reproduces the experimental data very well. In case of HERWIG the generated distributions are still lognormal and also obey the scaling, but some systematic deviation from the experimental results is seen. However I would like to stress that we did not tune the parameters of the models.

Figure 16 presents dispersions of various orders as functions of the average charge multiplicity. Again it is seen that JETSET reproduces experimental data very well. The points coming from HERWIG lie slightly above the experimental data, but follow the straight line which again proves the scaling.

The average charge multiplicity as a function of the collision energy $\sqrt{s}$ is plotted in the last figure. Average multiplicity coming from either generator obey the relation $\langle n_{ch} \rangle = \beta s^{\alpha} - 1$ (continuous line), but the values of parameters are slightly different from the fit to the experimental data (dashed line).

8 Conclusions

In conclusion I would like to say that in my opinion the present understanding of processes defining observed multiplicity distributions is quite good because the experimental data can be reproduced by Monte Carlo programs as well as by analytical calculations.

References

[1] G.Wrochna: "How to Fit the Lognormal Distribution", Warsaw University Preprint IFD/8/1990.

[2] R.Szwed, G.Wrochna and A.K.Wróblewski: "New AMY and DELPHI Multiplicity Data and the Lognormal Distribution", Warsaw University Preprint IFD/6/1990, to be published in Modern Physics Letters A.

[3] G.Wrochna: "Multiparticle production as a bivariate branching process", Warsaw University Preprint IFD/5/1990, to be published in Proceedings of the XIII Warsaw Symposium on Elementary Particle Physics, Kazimierz, Poland, May 1990.

[4] N.Arley and K.R.Buch: Introduction to the Theory of Probability and Statistics, New York 1950, Chapter 10, (John Wiley and Sons)

[5] R.Szwed, G.Wrochna and A.K.Wróblewski: Modern Physics Letters A 23 (1990) 1851.

[6] G.Ingelman, S.Carius: "Multiplicity Distribution from Cascade Processes", Uppsala University preprint TSL-ISV:32, to be published in the Proceedings of the XXVth Rencontres de Moriond "High energy hadronic interactions", Les Arcs, France, March 1990.

[7] R.Szwed, G.Wrochna and A.K.Wróblewski: "Scaling of Multiplicity Distributions and Collision Dynamics in e^+e^- and pp Interactions", Warsaw University Preprint IFD/7/1990.

[8] A.M.Polyakov: Sov. Phys. JETP 32 (1971) 296; 33 (1971) 850 (in Russian: Zh. Eksp. Teor. Fiz. 59 (1970) 542; 60 (1971) 296).

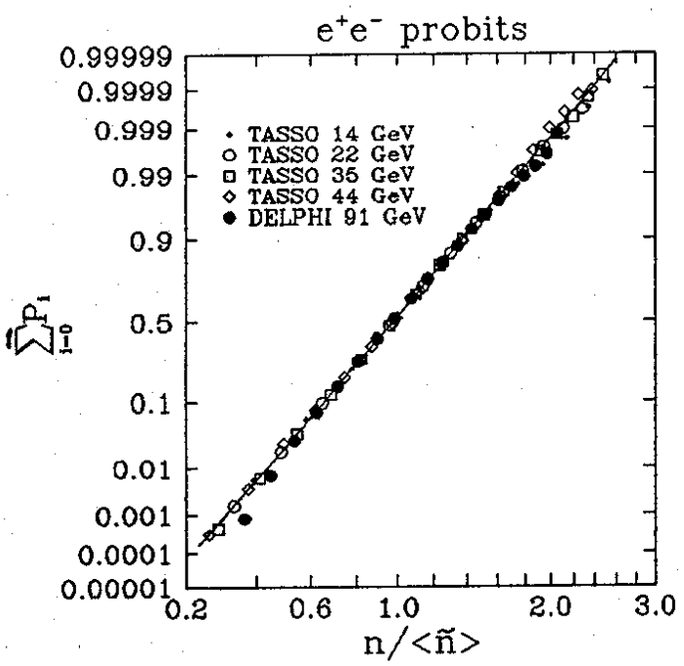

Fig. 1

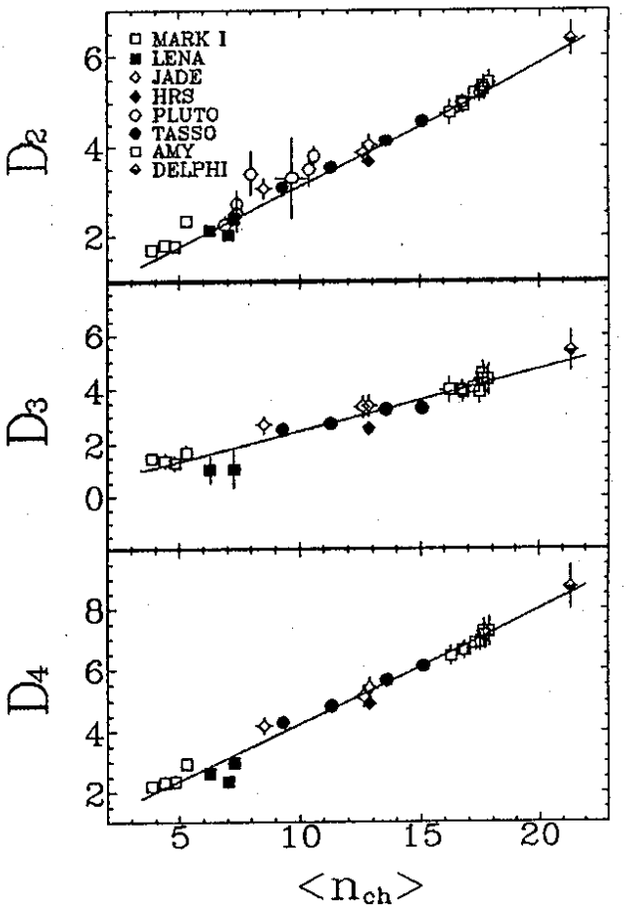

Fig. 2

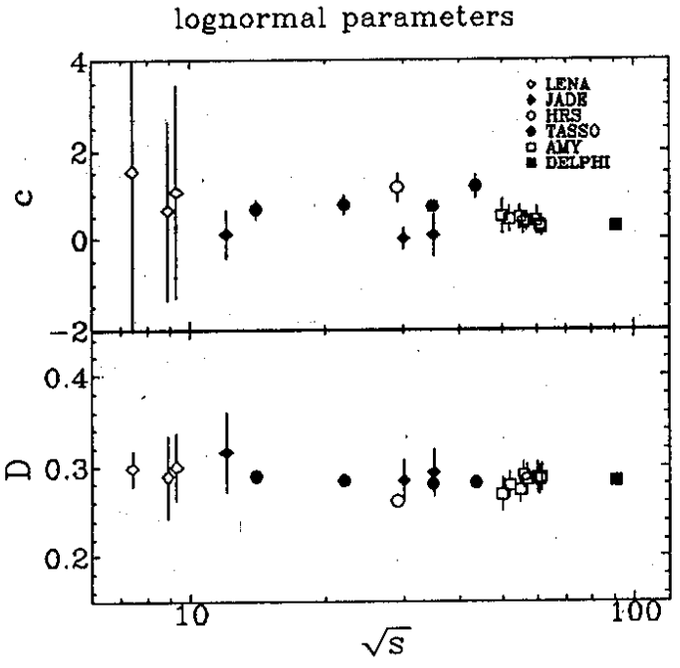

Fig. 3

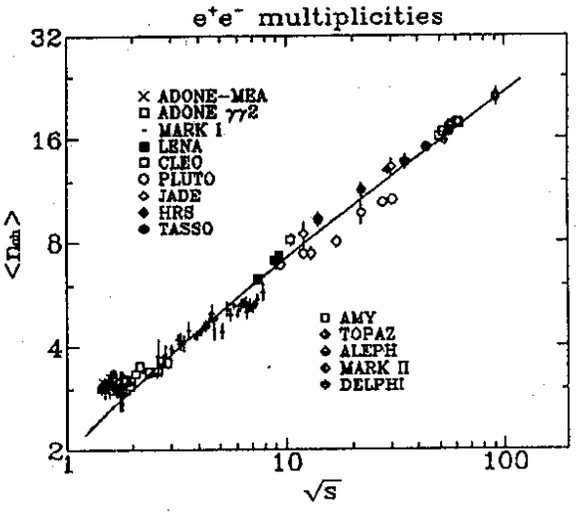

Fig. 4

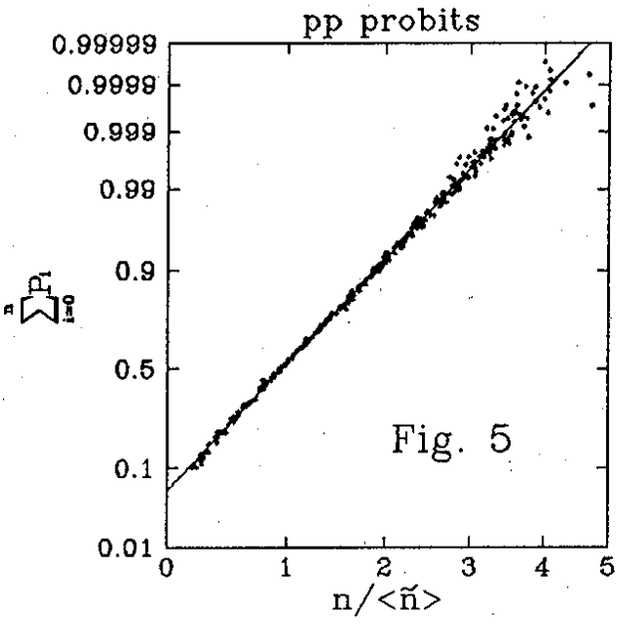

Fig. 5

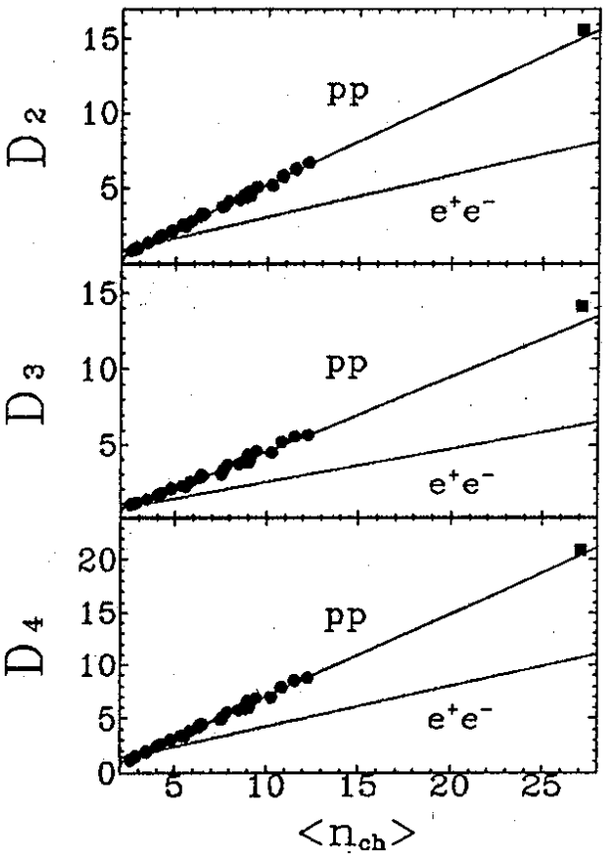

Fig. 6

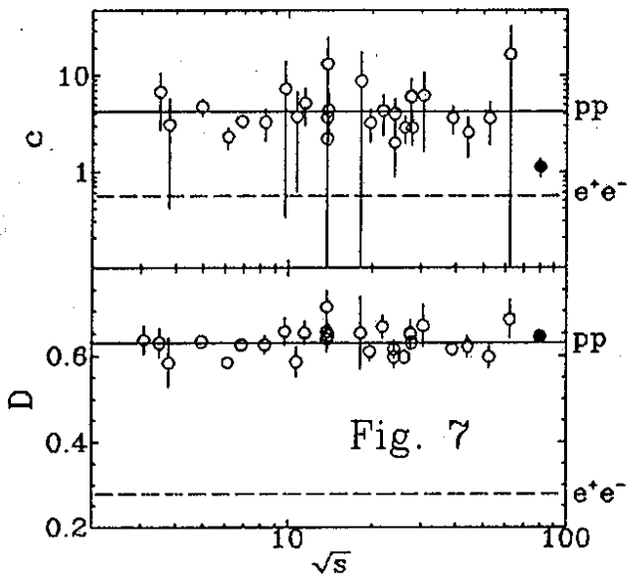

Fig. 7

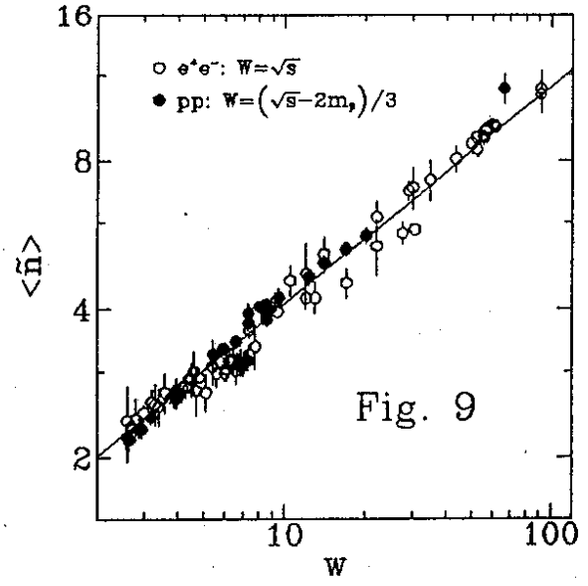

Fig. 9

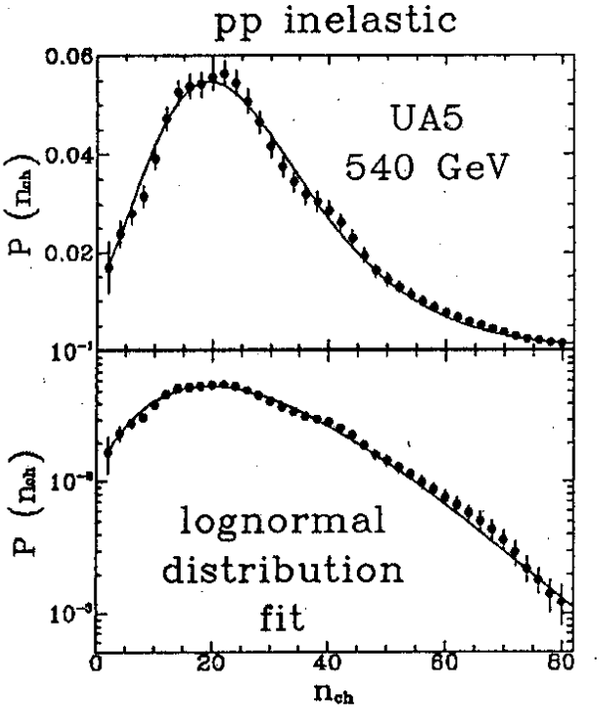

Fig. 8

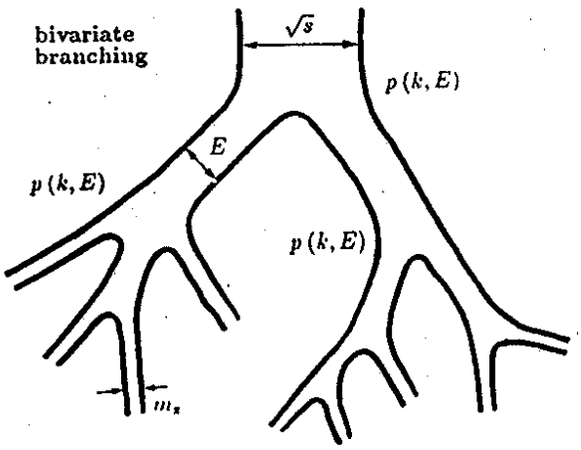

Fig. 10

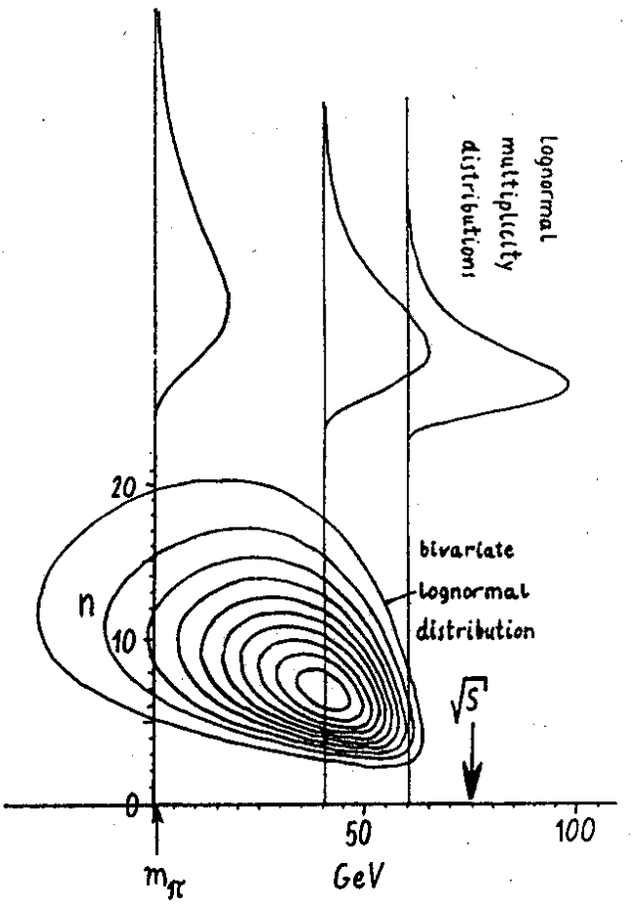

Fig. 11

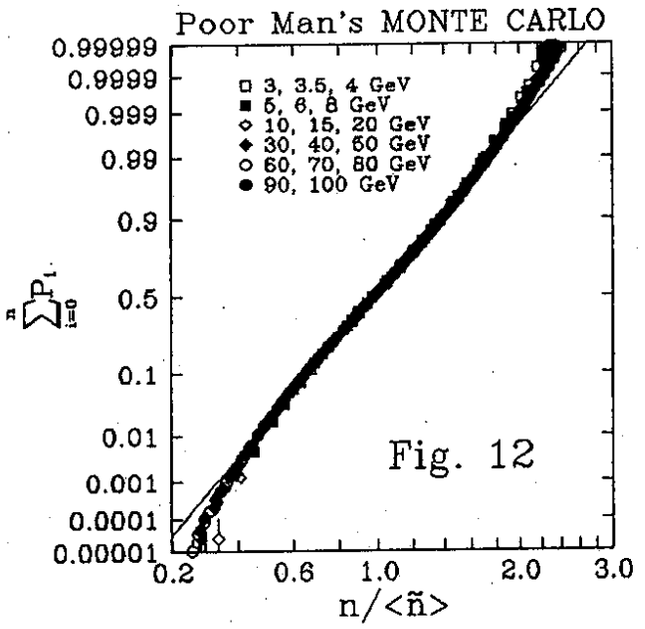

Fig. 12

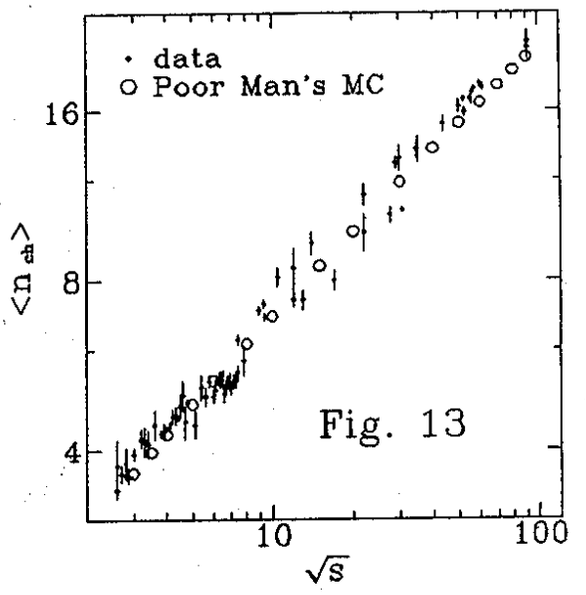

Fig. 13

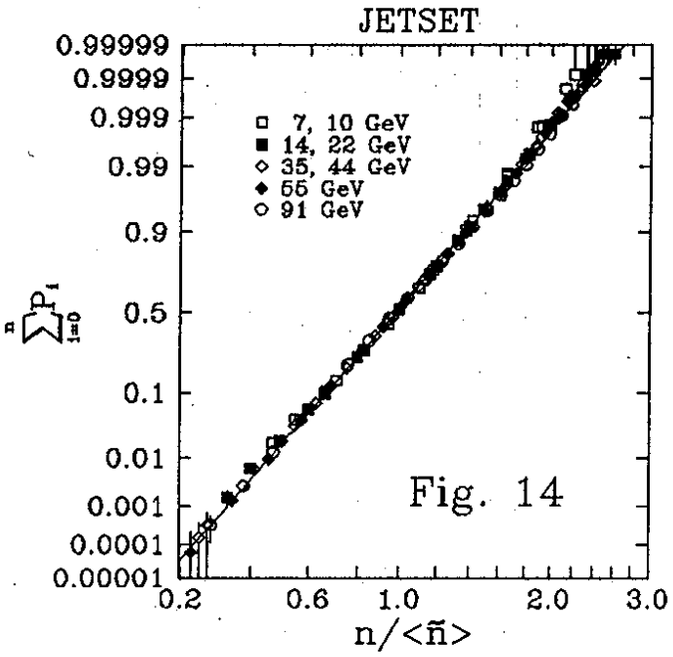

Fig. 14

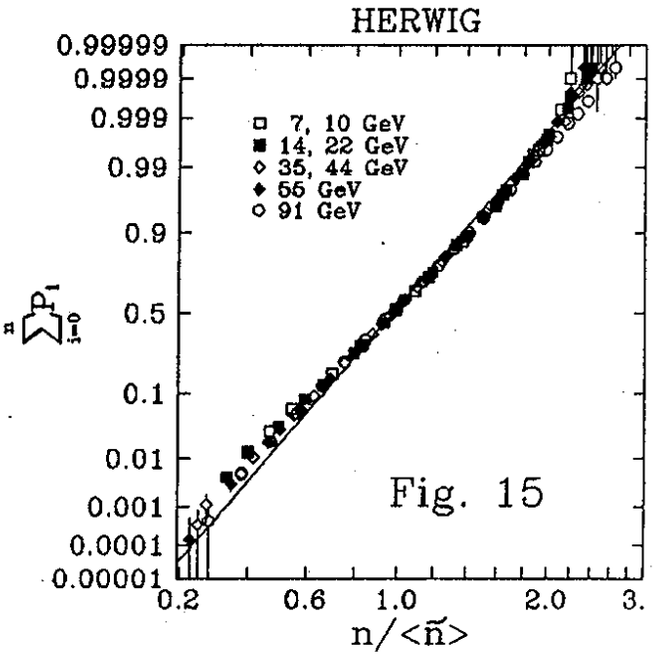

Fig. 15

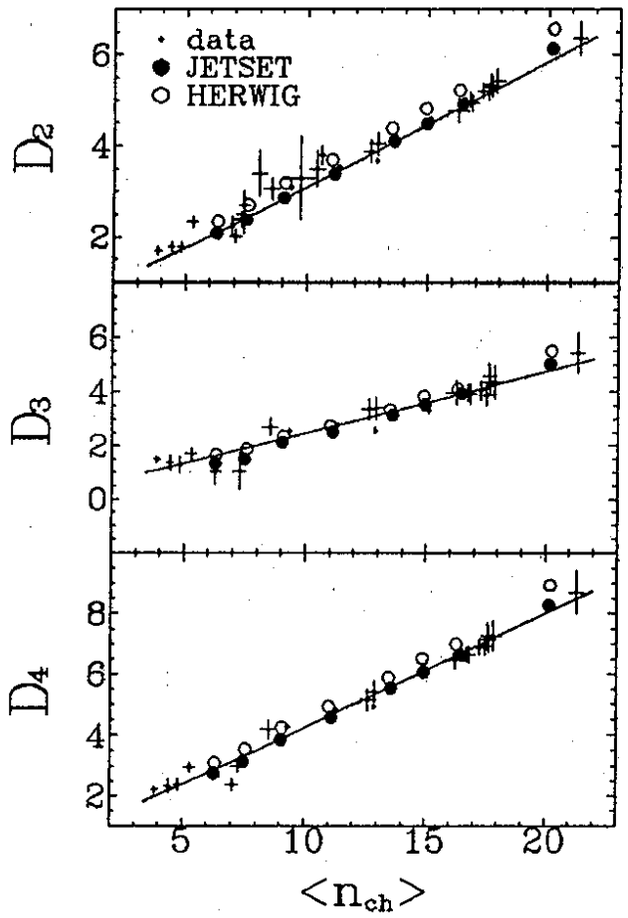

Fig. 16

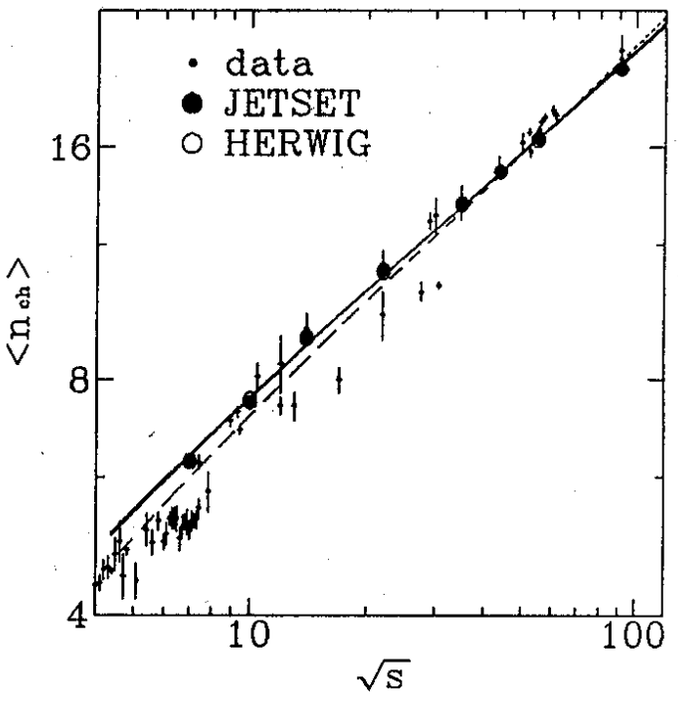

Fig. 17